

available at [www.sciencedirect.com](http://www.sciencedirect.com)journal homepage: [www.elsevier.com/locate/jmbbm](http://www.elsevier.com/locate/jmbbm)

## Opinion piece

# Indentation techniques for evaluating the fracture toughness of biomaterials and hard tissues

J.J. Kruzic<sup>a,\*</sup>, D.K. Kim<sup>b</sup>, K.J. Koester<sup>c</sup>, R.O. Ritchie<sup>c,d</sup>

<sup>a</sup> Materials Science, School of Mechanical, Industrial, and Manufacturing Engineering, Oregon State University, Corvallis, OR 97331, USA

<sup>b</sup> Department of Materials Science and Engineering, KAIST (Korea Advanced Institute of Science and Technology), Daejeon 305-701, Republic of Korea

<sup>c</sup> Materials Sciences Division, Lawrence Berkeley National Laboratory, Berkeley, CA 94720, USA

<sup>d</sup> Department of Materials Science and Engineering, University of California, Berkeley, CA 94720, USA

## ARTICLE INFO

## Article history:

Received 17 April 2008

Received in revised form

17 October 2008

Accepted 27 October 2008

Published online 12 November 2008

## ABSTRACT

Indentation techniques for assessing fracture toughness are attractive due to the simplicity and expediency of experiments, and because they potentially allow the characterization of both local and bulk fracture properties. Unfortunately, rarely have such techniques been proven to give accurate fracture toughness values. This is a concern, as such techniques are seeing increasing usage in the study of biomaterials and biological hard tissues. Four available indentation techniques are considered in the present article: the Vickers indentation fracture (VIF) test, the cube corner indentation fracture (CCIF) test, the Vickers crack opening displacement (VCOD) test and the interface indentation fracture (IIF) test. Each technique is discussed in terms of its suitability for assessing the absolute and relative toughness of materials or material interfaces based on the published literature on the topic. In general, the VIF and CCIF techniques are found to be poor for quantitatively evaluating toughness of any brittle material, and the large errors involved ( $\sim\pm 50\%$ ) make their applicability as comparative techniques limited. Indeed, indentation toughness values must differ by at least by a factor of three to conclude a significant difference in actual toughness. Additionally, new experimental results are presented on using the CCIF test to evaluate the fracture resistance of human cortical bone. Those new results indicate that inducing cracking is difficult, and that the cracks that do form are embedded in the plastic zone of the indent, invalidating the use of linear elastic fracture mechanics based techniques for evaluating the toughness associated with those cracks. The VCOD test appears to be a good quantitative method for some glasses, but initial results suggest there may be problems associated with applying this technique to other brittle materials. Finally, the IIF technique should only be considered a comparative or semi-quantitative technique for comparing material interfaces and/or the neighboring materials.

© 2008 Elsevier Ltd. All rights reserved.

\* Corresponding author. Tel.: +1 541 737 7027; fax: +1 541 737 2600.  
E-mail address: [jamie.kruzic@oregonstate.edu](mailto:jamie.kruzic@oregonstate.edu) (J.J. Kruzic).

## 1. Introduction

Accurately measuring the fracture toughness of brittle materials can often be challenging. Creating sharp pre-cracks can be difficult without catastrophically failing the specimen, while fracture toughness data using notched specimens can give erroneously high values (Munz et al., 1980; Ritchie et al., 1990; Fett and Munz, 2006). For those reasons, assessing fracture toughness by making direct measurements of cracks created using a sharp diamond indenter, such as Vickers, Knoop, Berkovich, or cube corner, can appear to be an attractive alternative to more traditional fracture toughness testing techniques (Lawn et al., 1980; Anstis et al., 1981; Fett, 2002; Fett et al., 2005). Such tests can be relatively quick and easy to perform, require little specialized equipment, and can allow probing of localized microstructural features. Accordingly, such techniques are finding considerable usage in studying the fracture behavior of biomaterials and hard tissues (Lopes et al., 1999; Kim et al., 2000; Marshall et al., 2001; Khor et al., 2003; Denry and Holloway, 2004; Imbeni et al., 2005; Mullins et al., 2007).

As with all fracture toughness testing techniques, the ultimate goal is to quantify the fracture toughness accurately in a way that can be universally compared with results generated using other techniques and from other studies. Unfortunately, techniques involving direct measurements from indent cracks are often unsuccessful in this regard (Li et al., 1989; Ponton and Rawlings, 1989b; Ghosh et al., 1996; Kruzic and Ritchie, 2003; Quinn and Bradt, 2007). A secondary goal may be to provide a quick semi-quantitative way to rank the toughness of different materials. In this case, indentation techniques can have some merit, but cannot be used indiscriminately. As will be discussed below, caution and good judgment are needed by the investigators, and large toughness differences are often needed to draw firm conclusions.

Accordingly, this article discusses some of the limitations of, and concerns with, using such indentation fracture techniques for studying biomaterials and biological hard tissues based on the published literature. Also presented are some new experimental results on using cube corner indentation to assess the fracture toughness of human cortical bone. Four techniques are discussed that involve making direct measurements of cracks emanating from indents. Techniques using indentation to create pre-cracks for traditional fracture toughness testing are not considered here. The techniques discussed include the Vickers indentation fracture (VIF) test, the cube corner indentation fracture (CCIF) test, the Vickers crack opening displacement (VCOD) test, and the interface indentation fracture (IIF) test.

## 2. Determining toughness from direct crack length measurements

### 2.1. Vickers indentation fracture (VIF) test

By far, the most widely used technique in the literature for assessing the fracture toughness directly from indent

cracks utilizes the Vickers indenter. First proposed in the late 1970's, this technique was developed to estimate the fracture toughness of ceramic materials by measuring the lengths of cracks emanating from Vickers indents (Lawn et al., 1980; Anstis et al., 1981). The method has subsequently received much recent attention for making measurements of fracture toughness in biomaterials (Lopes et al., 1999; Kim et al., 2000; Khor et al., 2003; Denry and Holloway, 2004). Lawn et al. (1980) modeled the elastic-plastic behavior under the indent, assuming that a median/radial crack system is created due to tensile stresses that form during unloading. They derived the expression:

$$K_c = \alpha \sqrt{\frac{E}{H}} \frac{P}{c^{\frac{3}{2}}} \quad (1)$$

where  $P$  is the applied load,  $E$  is Young's modulus,  $H$  is the hardness, and  $c$  is the length of the surface trace of the half penny crack measured from the center of the indent.  $\alpha$  is an empirically determined "calibration" constant, taken to be  $0.016 \pm 0.004$  based on a fit to experimental data using independent fracture toughness measurements (Anstis et al., 1981). A later model by Laugier (1985) derived a similar expression, with  $E/H$  raised to the  $2/3$  rather than  $1/2$  power and accordingly a different calibration constant. Published review articles on this method identify more than 30 different equations that have been presented in the literature for determining the fracture toughness from the length of the cracks observed on the sample surface (Ponton and Rawlings, 1989a; Quinn and Bradt, 2007), although most are not derived from physical models and are arrived at by curve fitting to data. Eq. (1) is generally the most cited and applied in practice and will be the focus of this discussion.

A quick review of Eq. (1), or other similar equations, reveals several causes for concern. First, an empirical calibration constant is used that has never been obtained, or justified, using physical models, and the standard deviation on the fit to obtain the calibration constant is large,  $\pm 25\%$ . Accordingly, at the 95% confident interval for all materials considered by Anstis et al. (1981), the toughness is only known to  $\pm 50\%$  even before scatter in experimental measurements is considered. Anstis et al. (1981) only included what they considered well behaved materials in their fit, and they point out anomalous glasses or softer ceramics as possible exceptional cases when this technique will be even less accurate. Subsequent evaluations of this technique have confirmed the large errors associated with this method (e.g., Fig. 1), and have found the error in toughness to exceed  $\pm 50\%$  in some cases (Li et al., 1989; Ponton and Rawlings, 1989b; Ghosh et al., 1996; Quinn and Bradt, 2007).

There are numerous potential sources that can contribute to such large errors, as there are many possible violations of the underlying assumptions of the model of Lawn et al. (1980), as well as issues such as R-curve and indentation size effects. The model assumes:

1. Two perpendicular well defined median/radial half penny cracks form below the indent during unloading due to the residual tensile stress field of the indent and,
2. The crack is, at the time of measurement, in equilibrium with that stress field, just at the stress intensity required to cause crack extension.

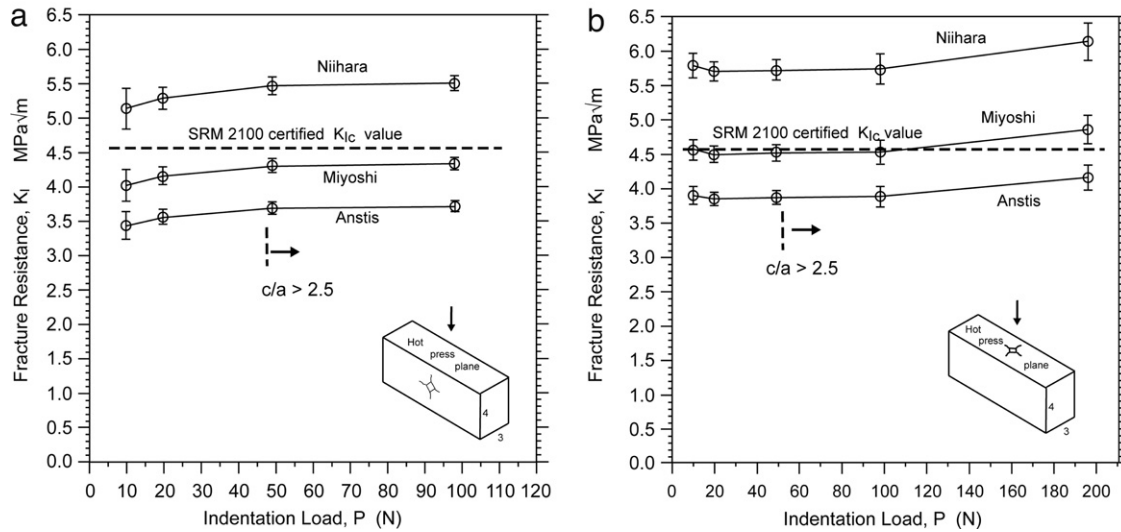


**Fig. 1 – Comparisons of VIF toughness results to the actual toughness for a  $\text{Si}_3\text{N}_4$  ceramic (SRM 2100) tested in two different orientations (see insets). Note the poor agreement between results for the three indentation equations evaluated (Anstis et al., 1981; Niihara, 1983; Miyoshi, 1985), while only in one case did the indentation toughness match the actual toughness. Similar results have been reported in many studies on many different ceramic materials, along with both increasing and decreasing apparent toughness with increasing indentation load (Li et al., 1989; Ponton and Rawlings, 1989b; Ghosh et al., 1996; Quinn and Bradt, 2007). Figure reproduced from Quinn and Bradt (2007).**

In some ceramics, indentation cracking is of the Palmqvist type which is difficult to discern from the half-penny crack when only viewing the surface trace; however, the analysis of Laugier (1987) concludes that this has little effect on the fundamental fracture toughness equations, provided the cracks are in equilibrium with the stress field. Another concern is that cracks are rarely found to initiate only upon unloading, except for the case of soda-lime glass, and instead often initiate during the loading portion of the indentation process (Cook and Pharr, 1990). This has the potential to disrupt the underlying residual stress field and affect the growth of the cracks during unloading. A further concern is the formation of other cracks that disrupt the residual stress field, such as lateral cracks or cone cracks, which are also commonly observed during Vickers indentation (Cook and Pharr, 1990; Kruzic and Ritchie, 2003). This is problematic since such cracks are not readily apparent to the experimentalist in opaque materials without post indent sectioning of the sample. Cook and Pharr (1990) reported that the details of indentation cracking phenomena are extremely material dependent, explaining a large part of why an accurate equation that can be applied for all brittle materials has not been achieved. Finally, in many brittle materials, sub-critical crack growth can occur after indentation, causing the cracks to extend. This will cause an erroneously low toughness value to be calculated using Eq. (1) that may approach the sub-critical crack growth threshold depending on (1) the time between indentation and measurement and (2) the testing environment. This problem can be mostly negated by testing in an inert environment such as silicone oil, but even trace amounts of water in the testing environment can affect the results.

Another issue is found for materials that exhibit rising fracture resistance with crack extension (i.e., rising R-curve).

For those materials, only one point on the R-curve is sampled by the indentation fracture test, and that point will depend on the load used unless the R-curve plateau has already been reached. Additionally, one of the parameters in Eq. (1),  $H$ , can depend on the indentation load.  $H$  generally decreases with increasing indentation load and this effect usually saturates after some critical load (Li et al., 1989; Quinn and Quinn, 1997). In some cases this effect can be trivial and easily avoided for carefully conducted fracture tests, such as in  $\alpha$ -SiC where the indentation size effect does not occur above  $\sim 3$ –5 N (Li et al., 1989; Quinn and Quinn, 1997). However, in other ceramics, this effect persists up to indentation loads as high as 100 N (Quinn and Quinn, 1997). The indentation size effect can result in an apparent higher measured toughness for higher indent loads (longer cracks) even if the toughness is not actually higher, giving erroneous rising R-curve-like results even in materials with no rising R-curve. Several researchers have reported apparent increases or decreases in toughness with increasing indent load using this technique, both in materials with no rising R-curve, such as  $\alpha$ -SiC and a ceramic glass, as well as for  $\text{Si}_3\text{N}_4$  ceramics that should be on the plateau of the R-curve at all indent sizes tested (Li et al., 1989; Ponton and Rawlings, 1989b; Ghosh et al., 1996; Quinn and Bradt, 2007). The fact that decreasing toughness has been observed indicates that several of the above factors play a role in the apparent change in toughness with indent load. Accordingly, using varying indentation loads to measure R-curves with the VIF toughness technique should not be considered an acceptable or accurate technique.

The original data of Anstis et al. (1981), and all the subsequent data from other critical reviews (Li et al., 1989; Ponton and Rawlings, 1989b; Ghosh et al., 1996; Quinn and Bradt, 2007), agree that this method produces large errors in the measured toughness, making the VIF method inaccurate

for comparisons to other techniques. For example, Li et al. (1989) reported the toughness of the  $\alpha$ -SiC that they examined by three different techniques to essentially be identical, while the VIF technique gave erroneous results.

Even as a simple comparative technique, the utility of the VIF test is severely limited. In the best case, the toughness could be determined at the 95% confidence interval within  $\pm 50\%$  of the actual value, and the reality may be worse based on some reviews of the technique. This implies that two materials with identical toughness may give a factor of three different toughness, or greater, by this technique. In their review, Ponton and Rawlings (1989b) give data for multiple cases where the actual toughness is incorrectly ranked by this technique, even among similar ceramics or ceramic glasses. In practice, when comparing mean VIF toughness values to detect statistically significant differences between materials, researchers must include not only the standard deviation from the crack length and hardness measurements, but also the standard deviation in  $\alpha$ . At the very least, the toughness values measured with this technique would need to be different by greater than a factor of three to consider drawing a conclusion that the toughness difference between the two materials is significant.

Based on all the information currently available on the VIF test, Quinn and Bradt (2007) concluded in their review that, "It should not be applied to or be acceptable for any basic fracture resistance measurements of ceramics or any other material". The present authors believe that, although this view may appear extreme, this is likely good advice that should be heeded by the community studying the mechanical behavior of biomaterials and hard biological tissues. The reasoning is that this technique is clearly inaccurate for measuring absolute toughness and, even as a comparative technique, this method can easily cause one to deduce incorrect conclusions with regard to the relative toughness of materials.

## 2.2. Cube corner indentation fracture (CCIF) test — Published literature

More recent studies have attempted to extend the use of Eq. (1) to sharper indentation geometries, such as the cube corner, by utilizing a different value of  $\alpha = 0.040$  (Pharr, 1998). The main advantage of this is that the threshold load to induce cracking is lowered significantly, generally by several orders of magnitude. This allows practitioners to induce cracking on very small size scales with micro and/or nano indentation instruments. Several recent studies have attempted to use this technique to assess the toughness of biological hard tissues such as cortical bone, enamel, and dentin (Marshall et al., 2001; Mullins et al., 2007). Pharr (1998) reports accuracy on the order of  $\pm 40\%$ ; however, a smaller number of calibration materials was used compared to the study of Anstis et al. (1981). Thus, one could expect that the smaller reported error is merely reflective of the fewer materials that were evaluated. Pharr (1998) comments simply that the accuracy of the CCIF technique is roughly similar to the VIF test. Accordingly, the discussion above on the accuracy of the VIF test for both absolute and comparative toughness measurements applies here as well.

To test the applicability of Eq. (1) to the CCIF test, Morris and Cook (2004) made *in situ* observations of cube corner indentations in soda-lime and fused silica glasses. They concluded that the residual stress field used to derive Eq. (1) was not responsible for the final crack configuration when using the cube corner indenter, raising a significant question as to the physical basis for applying Eq. (1) to the CCIF test. In their subsequent work, Morris et al. (Morris and Cook, 2005; Morris et al., 2005) proposed that, as indenters become more acute, a wedging load contributes a large part of the crack driving force, and that toughness estimates at small scales using acute indenters may be substantially in error due to the lack of equilibrium between the crack and the assumed dominant residual stress field. Thus, the generally similar accuracy of Eq. (1) for both the VIF and CCIF tests may be fortuitous, and clearly more study of the CCIF case is needed, as is suggested by Morris et al. (2005).

Mullins et al. (2007) have recently reported the measurement of the R-curve behavior of ovine cortical bone at very small crack lengths using the CCIF method. Those authors found that only a cube-corner indenter was sharp enough to initiate cracks in bone, and using applied normal loads of 0.05–3.0 N, they found crack lengths,  $c$ , of  $\sim 7$ –56  $\mu\text{m}$  (see Fig. 2). Using those measurements, they reported that the toughness of bone at those small crack sizes was  $\sim 0.5$ –2  $\text{MPa}\sqrt{\text{m}}$ , and thus was far lower than the normally reported (macroscopic) values of 3–7  $\text{MPa}\sqrt{\text{m}}$ , although very recent three-point bend tests on human cortical bone have shown toughness values of  $\sim 1$ –2  $\text{MPa}\sqrt{\text{m}}$  for the longitudinal orientation with crack sizes less than 500  $\mu\text{m}$  (Koester et al., 2008). As outlined above, there are many concerns about applying the CCIF technique to measure R-curves, which are compounded by the fact that bone is an organic/ceramic composite and dissimilar to the brittle materials for which the VIF and CCIF techniques are intended. As such, errors should be expected to be even larger than for brittle ceramics. Such concerns motivated the present authors to conduct additional experiments using the CCIF test on human cortical bone — the results are described in the next section.

## 2.3. CCIF test — New experiments on cortical bone

### 2.3.1. Materials and methods

These experiments were designed to examine the feasibility of generating indentation cracks in human bone and calculating indentation toughness values. Frozen human cadaveric cortical bone from the humerus of a 37 year-old male was sectioned to generate samples. Samples were sectioned from the mid-diaphysis cortex of the bone in two orientations; parallel (longitudinal, proximal-distal, orientation) and normal (transverse orientation) to the long axis of osteons using a low-speed saw. Two directions of the bone were examined in the current study to determine the importance of the orientation of the indent relative to the salient microstructural features of bone. For example, this enables the determination of whether the approach is feasible both when the preferred direction of cracking from the indentation corner is parallel to the cement sheaths, and when it is perpendicular to the cement sheaths. The sections were embedded in an epoxy resin with a low curing

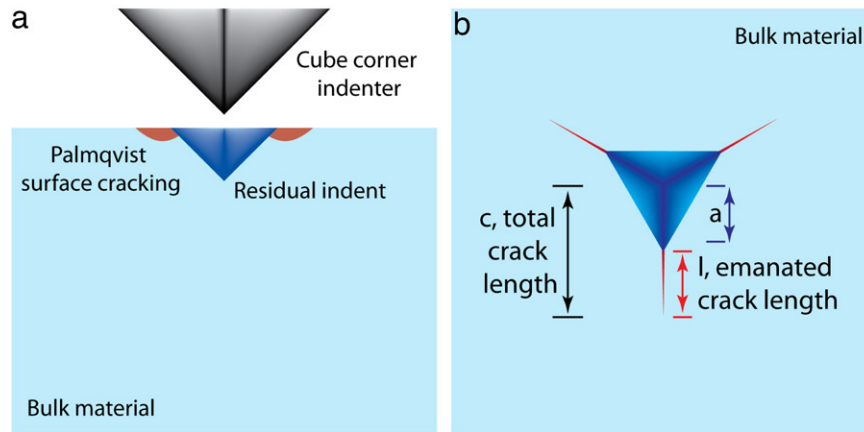


**Fig. 2 – Schematic diagrams of a cube-corner indenter and of the residual indent with surface cracks emanating from the indent corners. In (a), the indenter and material are shown in cross section to illustrate the type of cracking taking place. The two-dimensional surface view of the indentation is provided in (b). Labeled in (b) are the geometric parameters that are used in Eq. (1) to calculate toughness:  $a$  is the “contact radius”;  $c$  is the crack length; and  $l$  is the crack length emanating from the indent corner.**

temperature (Epoxicure™, Buehler) and allowed to cure overnight at room temperature. Following epoxy mounting, the samples were ground with SiC paper and polished with 0.05  $\mu\text{m}$  diamond slurry. Specimens were rehydrated by soaking in Hanks’ Balanced Salt Solution (HBSS) for at least 40 hr at room temperature. These procedures were chosen based on the reported success of Mullins et al. (2007) for ovine bone.

Indentations were carried out using a micro-hardness tester (1600–1000 Indenter, Buehler, Lake Bluff IL) with a cube-corner indenter, to a maximum load of  $\sim 3$  N. Samples were kept in HBSS until the time of testing and were indented immediately after removal from HBSS to ensure the samples were fully hydrated. Five indentations were made on each of the longitudinal and transverse sections with a cube-corner indenter. The indentation sites were imaged using a visible light microscope (Axiotech HD, Zeiss, Thornwood NY), with Nomarski differential interference contrast, to examine the indentation sites and the local microstructure of the bone. Following indentation, specimens were dehydrated using a series of ethanol solutions (Burr and Stafford, 1990); optical micrographs were also taken after dehydration to investigate whether this process had any effect on cracking at the indentation sites. The indentation sites were then examined in an environmental scanning electron microscope (ESEM) (S-4300 SE/N, Hitachi America, Pleasanton CA) to provide high-resolution images of the indentations at relatively high pressure,  $\sim 35$  Pa, and to minimize further dehydration *in vacuo*. Subsequently, the samples were sputter-coated with Au and a high-vacuum SEM (S-4300 SE/N, Hitachi America, Pleasanton CA) was used to determine the effect of *in vacuo* dehydration.

### 2.3.2. Results and discussion

Each corner of 10 indentations (30 total) was observed in two cross sections of human cortical bone. Indentation sites were observed in four different conditions: (i) as-indented (hydrated), (ii) as-dehydrated, (iii) in low vacuum (ESEM at 35 Pa), and (iv) in high vacuum (SEM at 0.2 mPa). This series

of conditions allowed the influence of each treatment of the bone on the indentation sites to be probed, *i.e.*, whether the dehydration itself could in any way induce, or influence, cracking at the corners of the indents.

Fig. 3 shows a cube-corner indent in the longitudinal section of human cortical bone made with a load of 2.89 N. Fig. 3 is representative of the other indents and indicates that cracks emanating from the indentation corners in bone are rare; a deep impression due to plastic deformation is evident, but few cracks emanate from the indent corners. In the rare occasion where small cracks were observed in the vicinity of the indent corner, as shown in Fig. 3(d, f), difficulties arose deducing whether these cracks were generated during indentation or were associated with pre-existing microcrack damage.

These conclusions generally pertain for indentations in bone, in both the longitudinal and transverse orientations. However, several other features can be seen at indentation sites in the transverse orientation, as shown in Fig. 4 where the indent is located near a Haversian system. The image shows an indentation that was on top of a pre-existing microcrack. A crack, that may be an indentation crack, can be seen near the indentation corner in Fig. 4(e); the location and direction of the crack at this indent corner is nearly along the cement line and the lamellar boundaries of a Haversian system, which are known to be weak interfaces and sites of preferential microcracking (Burr et al., 1988; Yeni and Norman, 2000). Cracks in the vicinity of the indent can be seen to widen during the ethanol and *in vacuo* dehydration process and, similar to the observations of other investigators (Rho et al., 1999), some new cracks formed as a result of dehydration (Fig. 4). It is unclear whether dehydration induced any cracking at the indentation corners, because the cracks at the indent corners were so small that they were only visible in the ESEM and SEM (Figs. 3 and 4).

Of the 30 separate indent corners that were examined, there were only 2 instances where a crack might reasonably be interpreted as an indentation crack. The length of the

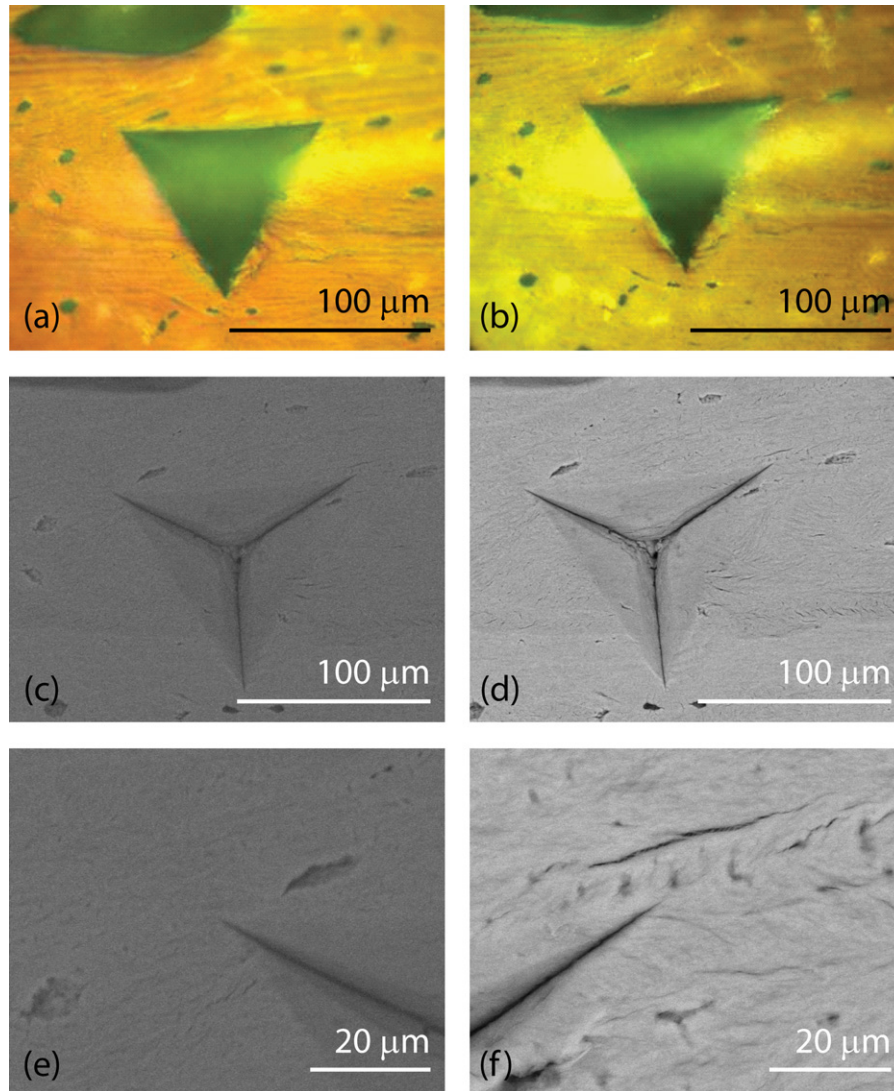


**Fig. 3 – Cube-corner indentation on the longitudinal section of human cortical bone made with a 2.89 N load. All micrographs show the same indentation site of the same sample with (a) as-Indented, (b) dehydrated, (c) ESEM, and (d) SEM. The higher magnification view (e) and (f) show the indent corners of (c) and (d), respectively. The crack near the top right corner of the indent could not be seen using only visible light microscopy.**

corner crack (measured from the indent corner) in Fig. 4(e) is about  $10\ \mu\text{m}$  and the parameters for calculation of fracture toughness using Eq. (1) are the indent size, the distance from center to corner,  $a = 55\ \mu\text{m}$ , and the crack size, the distance from center to crack tip,  $c = 65\ \mu\text{m}$ . Using these parameters and Eq. (1) gives an apparent toughness value of  $1.30\ \text{MPa}\sqrt{\text{m}}$ . It is important to note, however, that in the two cases where cracking was observed, it is believed that the cracks were too short for valid fracture toughness measurements to be made, even within the spirit of the CCIF technique, as discussed below.

With respect to the physical size of the indent cracks, when these cracks are small, the size of the plastic zone around the indentation becomes a limiting factor. The basis for relating contact radius to the plastic deformation around an indentation is the assumption that the strain field around an indentation is self-similar, and a change in contact area produces a corresponding change in plastic deformation. The

most widely accepted treatment of the plastic deformation around an indentation is the so-called “expanding cavity model”. The model deals with the expansion of the cavity as an incompressible hemispherical core of material subjected to an internal pressure. Here, the core pressure is directly related to the mean contact pressure. A direct relationship has been derived between the plastic zone radius,  $r_z$ , and the contact radius,  $a$ . The relationship is given by Johnson (1985):

$$\frac{E}{\sigma_Y} \tan \beta = 6(1 - \nu) \left( \frac{r_z}{a} \right)^3 - 4(1 - 2\nu), \quad (2)$$

where  $E$  is the elastic modulus,  $\sigma_Y$  is the uniaxial yield strength,  $\beta$  is  $90^\circ$  minus the semi-angle of the indenter, and  $\nu$  is Poisson's ratio. This equation was developed by assuming that the strain field around an indentation was self-similar such that,  $da/dr = a/r = m$ , where  $m$  is a constant. A study of many different materials with a wide range of material properties has shown that this method is

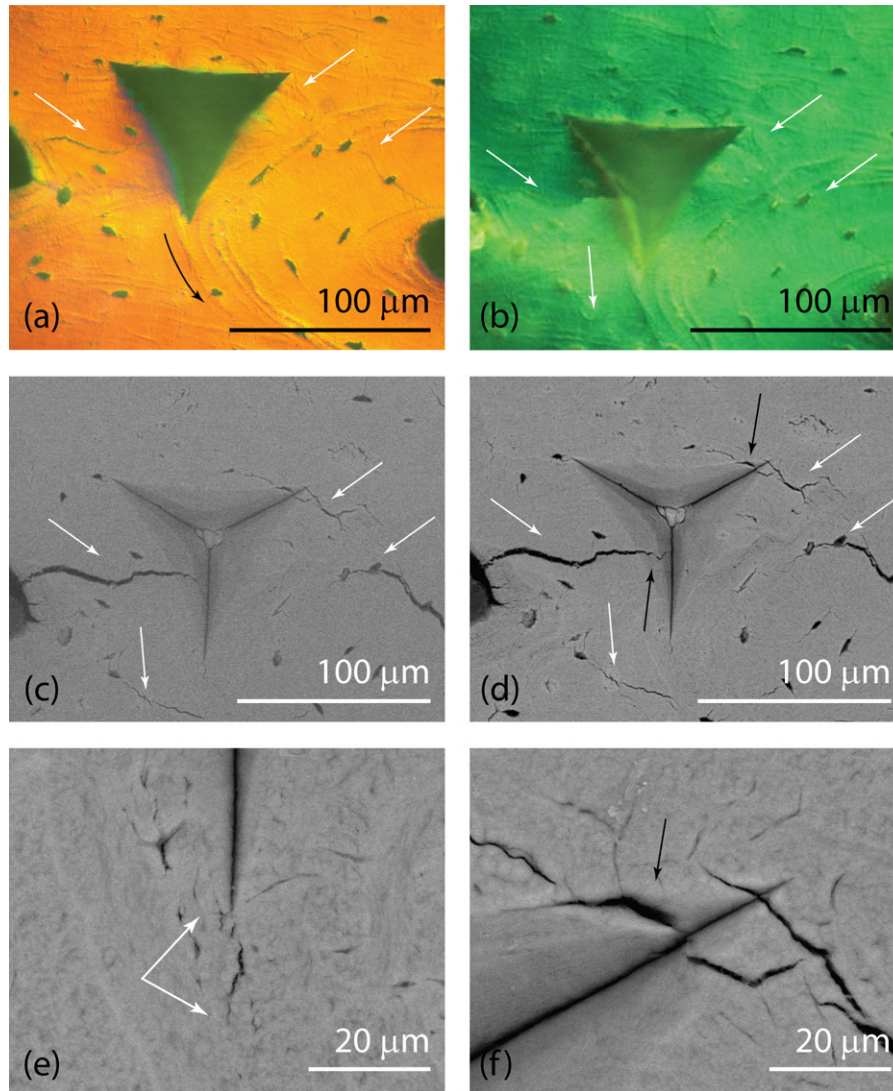


**Fig. 4 – Indentation site on the transverse section of human cortical bone. Images are of (a) as-Indented, (b) dehydrated, (c) ESEM, and (d) SEM. The bottom corner of the indentation, (e), shows a crack with  $l = 10 \mu\text{m}$ , which is one of the two cracks emanated from indent corners among 30 corners. High-magnification imaging of the top right corner, (f) revealed that no cracks were generated from this indent corner. The black arrows in (d) and (f) indicate the microcracks that were present before indentation. The black arrow in (a) indicates the local orientation of the cement line and the lamellar boundaries. The white arrows in (a–d) refer to the preexisting cracks in the vicinity of the indentation, and it can be seen from the images that these cracks widen between the fully hydrated state and the fully dehydrated state.**

appropriate for many materials (Kramer et al., 1998). For fully plastic materials, the ratio of plastic-zone radius to contact radius,  $r_z/a$ , is  $\sim 2.5$ . When the above treatment is applied to the cube-corner indentation of cortical bone, assuming  $E = 12 \text{ GPa}$ ,  $\sigma_Y = 300 \text{ MPa}$ , and  $\nu = 0.2$ , the plastic-zone radius to contact radius ratio,  $r_z/a$ , is  $\sim 2.3$ .

With the few cracks emanating from indents in bone in our experiments, and those of Mullins et al. (2007), which are at maximum in the range of 5 to  $10 \mu\text{m}$  (measured from the corner of the indent), the ratio of the total crack size to the indent impression,  $c/a$ , is  $\sim 1.1$ , which suggests that any small cracks emanating from an indentation corner in bone will be deeply embedded in the plastic zone, as shown in Fig. 5. Thus, an additional problem exists here as to the validity of applying linear elastic fracture mechanics (LEFM) in any form

to these small cracks that is completely separate from the normal inaccuracies of the CCIF technique described above.

Two samples from one individual were tested in this study, and indentation cracks only formed in the immediate vicinity of cement sheaths or lamellar boundaries, i.e., at weak interfaces within the microstructure, which may be why the incidence of indent cracking was so low. As such, it is important to point out that there are several factors, e.g., local mineralization, age, history, etc., which could have influenced the amount of cracking at the indentation sites. Due to the small number of samples examined, these experiments do not definitively show that in all cases the same amount of cracking will be observed. However, if the amount of cracking in this study and in Mullins et al. (2007) is representative, than the cracks are much too small to measure toughness using a

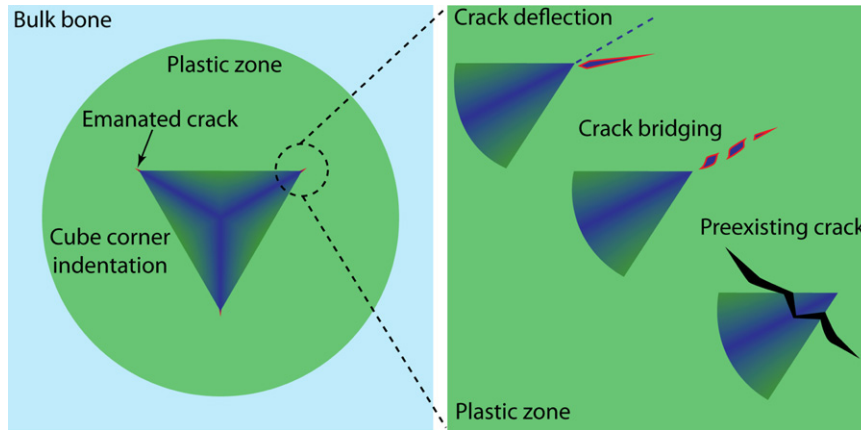


**Fig. 5 – Schematic diagram of an indentation in bone with the indent, emanated crack length, and approximate plastic-zone size shown to scale. Also illustrated are the various crack configurations that are observed at the corners of the indentations, namely crack deflection, crack bridging and indentation on top of pre-existing cracks. As seen in Fig. 4(e), crack bridging was present when a crack grew off of the indent and the extent of this extrinsic toughening mechanism was rather large compared to the emanated crack length. This is attributable to the crack length being on the same scale as some of the microstructural elements in bone. In some instances, the indent was made on top of pre-existing damage. It is likely that when an indent is made on pre-existing damage, the residual stresses at the indent are diminished and there is a decreased likelihood of indentation cracking.**

LEFM based technique. In addition to the plastic zone of the indent, the local plasticity associated with the crack tip itself would be expected to be on the same size scale as the crack size, which is another violation of LEFM.

This problem is confounded by the ubiquitous presence of microcrack damage, as *in vivo* bone contains a distribution of diffuse nano- and micro-scale cracks. While confusing pre-existing cracks with those formed by indentation may be avoided with careful experimentation, such damage may affect the local modulus in Eq. (1) and the residual stress field presumed by Eq. (1) to be driving the crack.

These reservations specific to bone are summarized in Fig. 5, in terms of a schematic illustration of an indentation in bone with the associated plastic zone (estimated from Eq. (2)) and some factors that diminish the ability to conduct indentation toughness measurements in bone.

### 3. Vickers crack opening displacement (VCOD) test

The VCOD method was developed by Fett et al. for evaluating fracture toughness directly from measurements of the crack opening displacements (CODs) of Vickers indent cracks (Fett, 2002; Fett et al., 2005). With this method, by fitting the measured crack-opening profile to the expected profile for a Vickers indentation crack, the stress intensity at the crack tip may be determined. Crack-opening profiles may be measured in a scanning electron microscope (SEM) or atomic force microscope (AFM). Fett has developed both rigorous and approximate solutions for the crack opening displacements, based on basic assumptions similar to Lawn et al. (1980) given in Section 2.1.

One approximate solution has the form (Fett, 2002; Fett et al., 2005):

$$u(r) = \frac{4K_{tip}\sqrt{a}}{\pi E'} \left( A\sqrt{1-\frac{r}{c}} + B\left(1-\frac{r}{c}\right)^{\frac{3}{2}} + C\left(1-\frac{r}{c}\right)^{\frac{5}{2}} \right), \quad (3)$$

where  $E'$  is the plane strain modulus (i.e.,  $E' = E/(1-\nu^2)$ , where  $\nu$  is Poisson's ratio) while  $r$ ,  $a$ , and  $c$  are the radial position, contact-zone radius, and the crack length, respectively, as measured from the center of the indent. The coefficients are written as:

$$A = \sqrt{\frac{\pi c}{2a}} \quad (4)$$

$$B \cong 0.011 + 1.8197 \ln\left(\frac{c}{a}\right), \quad (5)$$

$$C \cong -0.6513 + 2.121 \ln\left(\frac{c}{a}\right). \quad (6)$$

Note that the first term in Eq. (2) reduces to the familiar Irwin elasticity relationship for a near-tip crack-opening profile:

$$u(r) = \frac{K_{tip}}{E'} \sqrt{\frac{8(c-r)}{\pi}}. \quad (7)$$

There are several important points to make about this formulation in comparison to the VIF technique. First, Fett needed no empirical calibration to formulate the expressions for the CODs. Secondly, the hardness is not part of the formulation, erasing any concerns about the indentation size effect. Finally, because the technique evaluates the crack tip toughness, for materials with rising R-curves, it should always evaluate the same point on the R-curve, the initiation or intrinsic toughness.

This method has proven to be quite successful in quantifying the toughness of glasses. Fett et al. (2004, 2005) were able to accurately measure the subcritical cracking threshold for a soda-lime glass using this technique. Burghard et al. (2004) used both this technique and the Anstis et al.

(1981) VIF method described above to evaluate the toughness of a soda-lime glass and a borosilicate anomalous glass. Both of these glasses are known to have identical fracture toughness by conventional double cantilever beam fracture toughness measurements. They found that, while the Anstis VIF method gave more than twice the actual toughness for the borosilicate glass, the method of Fett gave identical, and correct, toughness values for the two glasses.

The success of studies using soda-lime glass is not too surprising considering such glasses have been observed to have nearly ideal median/radial indentation cracking behavior with respect to the model, with no cracks observed during loading, and the entire cracking process driven by the residual stresses during unloading (Cook and Pharr, 1990). Although additional lateral cracking was observed by Cook and Pharr for their particular soda-lime glass, that was not reported by Burghard et al. (2004) or Fett et al. (2004, 2005). Thus, this represents the ideal system to utilize this technique.

For borosilicate glass, the cracking behavior is generally not so ideal for this technique. During loading, Cook and Pharr (1990) observed cone cracks form first, followed by radial cracks. Then, during unloading, the radial cracks grow due to the residual stresses, and lateral cracks formed as well. Both the cone and lateral cracks may be expected to relax the assumed residual stress field and affect the equilibrium COD. Burghard et al. (2004) reported morphologically different indent cracks for their borosilicate glass, relative to their soda-lime glass; however, the technique of Fett seems to be accurate for both glasses nonetheless. This is probably because the median/radial cracks extended considerably beyond any other cracks into the residual stress field of the indent, perhaps making the effects of the other cracks negligible.

Only one study has applied this technique to crystalline ceramics, and the results were not as encouraging. Kruzic and Ritchie (2003) found poor agreement between the measured crack-opening shapes and those predicted using Eqs. (3)–(6) for an  $\alpha$ -SiC ceramic. Furthermore, fitting the near tip region to the Irwin relation (Eq. (7)) revealed that the crack opening was much less than expected, considering the toughness of the material. Those researchers made observations of secondary radial cracks and subsurface lateral cracks (Fig. 6), both of which may have relieved some residual stress and decreased the crack openings. Such results are not entirely surprising as Cook and Pharr (1990) reported cracking sequences and patterns in crystalline materials to be very different from glasses, with radial cracks forming immediately upon first loading. In general, they found the cracking behavior of soda-lime glass, which is ideal for this method, to be the exception, and not the rule. Thus, while this method holds promise for application to glasses, caution should be used when attempting to extend it to other materials, or even other glasses where the cracking patterns or sequences are considerably different from soda-lime glass.

#### 4. Interface indentation fracture (IIF) test

Another approach that uses indentation cracks to assess fracture toughness is intended for use on material interfaces,

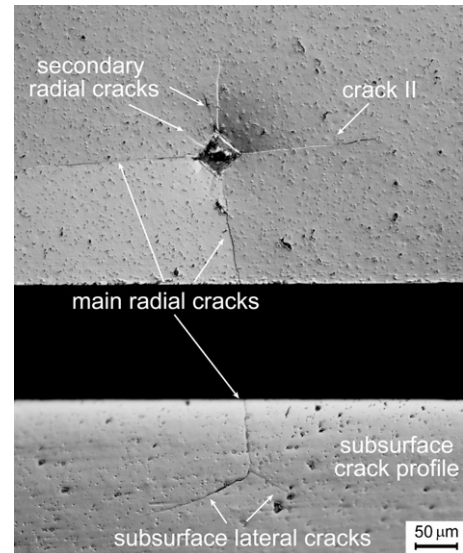


**Fig. 6 – Optical micrographs showing a Vickers indent in  $\alpha$ -SiC from Kruzic and Ritchie (2003) with the subsurface crack profile of one of the main cracks. Crack II was used for crack-opening profile measurements prior to sectioning. Clear evidence of subsurface lateral cracking and secondary radial cracking are seen, which likely affected the crack-opening profiles. Figure reproduced from Kruzic and Ritchie (2003).**

namely the qualitative technique developed by Becher et al. (1996). This method uses many indents to create cracks that impinge on a material interface with various angles of incidence, and yields largely comparative results. For example, by noting the critical angle of incidence that causes interfacial debonding, one can have a comparative measure of the toughness of several different interfaces. Relatively weak interfaces will debond even at high angles of incidence,  $\theta$ , up to  $90^\circ$ , while interfaces with relatively high fracture resistance will require lower angles to induce debonding (Fig. 7(a)). This allows, for example, one to compare the toughness of similar interfaces created using slightly different processing conditions, or with variations in interfacial chemistry.

A slight variation of this approach allows one to put a lower bound on the toughness of the interface. For example, such a study was carried out for the dentin-enamel junction (DEJ) in human teeth by placing indents in the enamel with cracks impinging on the DEJ (Imbeni et al., 2005). In that study, it was noted that the majority of cracks had an angle of incidence on the DEJ near  $90^\circ$  since cracking in the enamel occurred by separation of the enamel rods, which are oriented perpendicular to the DEJ. Furthermore, nearly all cracks were observed to penetrate the DEJ (Fig. 7(b)). Conditions for a crack to penetrate a material interface at  $90^\circ$  have been determined by He and Hutchinson (1989) as a function of the elastic properties of the materials on each side. In the case of the DEJ, it was determined that the interface must have a critical strain energy release rate,  $G_c$ , of at least 75% that of the dentin to not experience debonding with a  $90^\circ$  angle of incidence.

It is important to note that one cannot expect to get a definitive interface toughness value using these methods.

**Fig. 7 – (a) Schematic illustration of a Vickers indent used to determine the critical angle of incidence that causes debonding of an interface. By plotting the debond length,  $l_{db}$ , as a function of the incident angle,  $\theta$ , one can determine the critical angle for debonding, which allows comparisons of interfacial toughness between similar material systems. (b) SEM micrograph of a crack emanating from a Vickers indent in enamel and propagating into dentin in a human molar tooth by penetrating the dentin-enamel junction (Imbeni et al., 2005).**

These methods are only semi-quantitative at best, and are used for comparative purposes, i.e., to compare the toughness of similar interfaces, or the toughness of the interface with the neighboring material. One should not compare interfaces between different material systems, as the debonding behavior will also be affected by the elastic properties of the materials, the indentation cracking pattern/sequence, the indent load, etc. In general, one must take care to use a single indent load, and to consistently control the position of the indent, for example to ensure that the ratio of the intersecting crack length,  $l_{int}$ , to the nominal crack length,  $l_0$ , is kept approximately constant, e.g.,  $l_{int}/l_0 \sim 0.5$  (Fig. 7(a)). Erroneously placed indents, i.e. indents not meeting such criteria, should not be included in data collection.

## 5. Additional Considerations for Biomaterials and Hard Tissues

Generally, it is most interesting to understand the fracture behavior of biomaterials and hard tissues in their hydrated states. Accordingly, one must be careful when choosing examination methods to observe cracks in these materials. For example, desiccation in a high, or even low, vacuum scanning electron microscope (SEM) may cause spontaneous cracking at sharp stress concentrators, such as one finds around indents, or even interfaces such as the DEJ (Imbeni et al., 2005). Thus, just because one observes cracks in an SEM, care must be taken to ensure such cracks are not an artifact of the desiccation process, and independent verification should be performed using other techniques such as optical microscopy and/or environmental SEM, as was done by Imbeni et al. (2005).

Next, many hard tissues, bioceramics, and biocomposites, exhibit rising fracture resistance with crack extension, e.g., Kruzic et al. (2003), Vashishth (2004) and Nalla et al. (2005). In those cases, fracture resistance should be expressed

as a fracture resistance curve (R-curve) which, in turn, governs the strength of the material. As described above, the ability of indentation techniques to accurately quantify  $K_{Ic}$  for materials with a single value of toughness is questionable. Moreover, in no case have researchers successfully measured an R-curve using one of the above indentation techniques and shown agreement with a conventionally measured R-curve. Accordingly, one should use appropriate skepticism (Kruzic and Ritchie, 2008) when interpreting results of studies that claim to measure R-curves using indentation methods, (e.g., Mullins et al. (2007)).

Finally, hard tissues are dissimilar to the ceramic materials for which indentation fracture testing is intended. All hard tissues have an organic component, which is a significant volume fraction in bone and dentin. As originally cautioned by Anstis et al. (1981), applying such techniques to softer materials should be expected to introduce even larger errors than normally found for brittle ceramics, and in cases where cracking does not extend well out of the plastic deformation zone of the indent there is certainly not a valid justification for using a linear elastic fracture mechanics based technique.

## 6. Conclusions

Based on a review of the current literature on the Vickers indentation fracture (VIF) test, the cube corner indentation fracture (CCIF) test, the Vickers crack opening displacement (VCOD) test, and the interface indentation fracture (IIF) test, along with new CCIF experiments on human cortical bone, it is concluded that:

1. Classical indentation toughness measurement methods, which use the size of cracks emanating from Vickers or cube corner indents to determine the toughness, have been seeing growing popularity for measuring the toughness of biomaterials and hard biological tissues. Unfortunately, these methods are generally unsuitable for



